Hardware-in-the-Loop Simulation of a Virtual Synchronous Motor

Mihailo Tanasić
School of Electrical Engineering
University of Belgrade
Belgrade, Serbia
tm213085m@student.etf.bg.ac.rs

Bogdan Brković
School of Electrical Engineering
University of Belgrade
Belgrade, Serbia
brkovic@etf.bg.ac.rs

Milovan Majstorović
School of Electrical Engineering
University of Belgrade
Belgrade, Serbia
majstorovic@etf.bg.ac.rs

Leposava Ristić
School of Electrical Engineering
University of Belgrade
Belgrade, Serbia
leposava.ristic@etf.bg.ac.rs

***Abstract*— In this paper, the operation of a three-phase active rectifier controlled as a virtual synchronous machine is presented and developed on a hardware-in-the-loop platform. The relevant rectifier control algorithm variables, such as grid currents or virtual electromagnetic torque, exhibit transient responses in accordance with the mathematical model of a synchronous machine. The reactive power is maintained at zero to achieve unity power factor over a wide range of output voltage references. The aforementioned behavior is confirmed using a hardware-in-the-loop device which simulates responses of all hardware elements of the electrical circuit. The control algorithm is implemented on an FPGA-based controller board which is used to acquire measurements and generate PWM signals.**

Keywords—three-phase PWM active rectifier, control algorithm, virtual synchronous machine, hardware-in-the-loop

I. Introduction

The increased presence of renewable energy sources (RES) in power systems during the 21st century is the result of the continuous growth of energy consumption and the reduction of fossil fuel reserves, combined with the deterioration of the environment due to fossil fuel exploitation. The importance of RES is asserted through plans for increase in the total share of such energy sources in the production of electricity. In accordance with most leading countries in the world it is predicted that by 2050 up to 30% of the total electricity production will be from renewable sources [1]. In this way, hybrid systems are formed, in which electricity production is based on a combination of conventional and renewable energy sources. Although fundamentally good, this approach creates new problems for the electric power system, but also for consumers [2].

High-power synchronous generators, which are characterized by their large rotor masses, are favorable in terms of system stability as they increase its overall inertia. As such, they are directly connected to the grid. On the other hand, integration of renewable sources into the grid requires the use of grid-side converters. These converters typically incorporate current, power, and DC-link voltage controllers. They are tuned to have a fast response and good dynamic characteristics. The nature of these controllers is such that an increase in grid voltage results in a decrease in converter current and vice versa. They are adjusted to maintain the required power of load at the output and this type of behavior adversely affects the stability of the grid, especially in the case of a significant share of such converters in the grid [2, 3]. In recent years, solutions for the control of grid converters based on the equations of the synchronous machine have become popular. Such a converter is called a virtual synchronous machine (VSM) [1, 4, 5, 6]. The idea is that VSM emulates the existence of inertia and thus imitates the dynamics of synchronous machines when transients occur in the grid, thereby stabilizing voltage and frequency. This type of converter, usually referred to as a virtual synchronous generator (VSG), essentially represents a grid-side inverter. However, such solutions related to power rectifiers are also used. Reactive power control provides the ability to operate with unity power factor, which is a characteristic of active rectifiers. This paper deals with an active rectifier controlled as a synchronous machine in motor operation mode, better known as a virtual synchronous motor [7].

In this paper, the operation of a three-phase active rectifier controlled according to the equations of a synchronous machine is analyzed. The control algorithm is verified using a hardware-in-the-loop (HIL) device that allows testing without actual hardware elements (transistors, load, grid connection, etc.) that are instead simulated in real time. However, the control unit is still an actual controller board that communicates with simulated hardware.

Following the first section, this paper is organized as follows: Section II describes the synchronous machine mathematical model which is a core element of the VSM control algorithm; main parts of VSM are established in Section III; fourth section describes the setup used to verify control of power converter in real time environment with brief explanation of the applied equipment. Results of HIL simulations are provided in the fifth section, followed by conclusions, given in the final section.

II. Synchronous Machine Mathematical Model

Let us consider a three phase, two-pole non-salient pole synchronous machine. It is assumed that stator windings have a sinusoidal distribution, although they are graphically displayed as concentrated in Fig. 1. Following derivation is based on [8] with adopted motor operating mode.

979-8-3503-4317-5123/$31.00 ©2023 IEEE

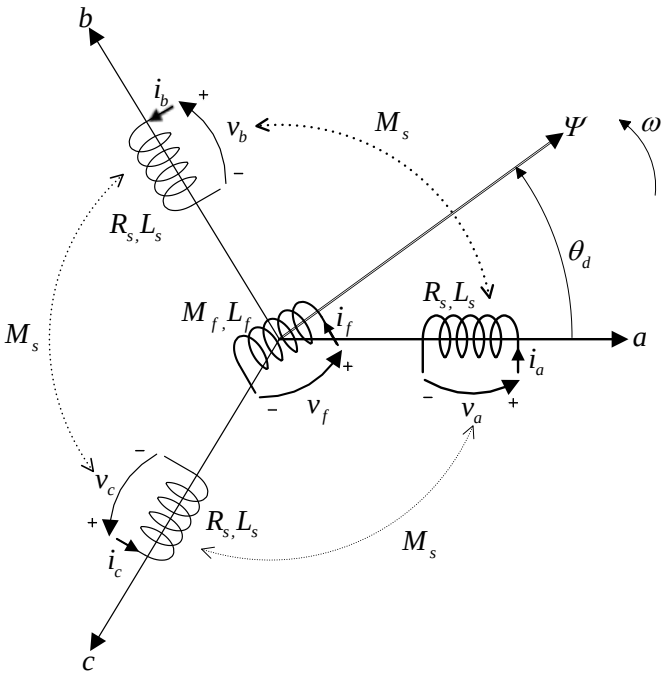

Fig. 1. Synchronous machine model

Angle θ_d defines the rotor position with respect to the reference axis of stator,

$$\theta_d = \omega t + \theta_{d0}\,, \tag{1}$$

where ω represents the rotor angular velocity, and θ_{d0} defines the initial position of the rotor. Mutual inductances of stator and rotor windings are time dependent and can be modeled as:

$$L_{af} = M_f \cos(\theta_d) \tag{2}$$

$$L_{bf} = M_f \cos(\theta_d - 120^\circ) \tag{3}$$

$$L_{cf} = M_f \cos(\theta_d - 240^\circ)\,. \tag{4}$$

It is now possible to define flux linkages of each winding as:

$$\lambda_a = L_{aa} i_a + L_{ab} i_b + L_{ac} i_c + L_{af} i_f \tag{5}$$

$$\lambda_b = L_{ba} i_a + L_{bb} i_b + L_{bc} i_c + L_{bf} i_f \tag{6}$$

$$\lambda_c = L_{ca} i_a + L_{cb} i_b + L_{cc} i_c + L_{cf} i_f \tag{7}$$

$$\lambda_f = L_{af} i_a + L_{bf} i_b + L_{cf} i_c + M_f i_f\,. \tag{8}$$

Self-inductances of stator windings are denoted as $L_{aa}=L_{bb}=L_{cc}=L_s$, mutual inductances between stator windings are denoted as $L_{ab}=L_{bc}=L_{ac}=-M/2$, while i_f denotes field winding current. The following equation describes the instantaneous value of stator winding voltage,

$$v_x = R_s i_x + \frac{d\lambda_x}{dt} \tag{9}$$

for $x \in \{a,b,c\}$ where R_s describes stator winding resistance, as well as

$$i_a + i_b + i_c = 0\,, \tag{10}$$

in case of isolated neutral, while back-emf equations can be obtained for each phase according to (14) – (16).

$$e_a = -M_f i_f \omega \sin(\theta_d) + M_f \frac{di_f}{dt}\cos(\theta_d) \tag{14}$$

$$e_b = -M_f i_f \omega \sin(\theta_d - 120^\circ) + M_f \frac{di_f}{dt}\cos(\theta_d - 120^\circ) \tag{15}$$

$$e_c = -M_f i_f \omega \sin(\theta_d - 240^\circ) + M_f \frac{di_f}{dt}\cos(\theta_d - 240^\circ) \tag{16}$$

Steady-state current i_f is constant, thus, the second element in (14)-(16) can be neglected. These equations are of tremendous importance for VSM since they present voltage references for pulsed modulation.

Energy that has been accumulated in the machine magnetic field is a sum of both rotor and stator fields [4].

$$W = \frac{1}{2}(i_a\lambda_a + i_b\lambda_b + i_c\lambda_c) + \frac{1}{2} i_f \lambda_f \tag{17}$$

The first derivative of W with respect to angular (mechanical) position multiplied by the number of pole pairs equals electromechanical (rotating) torque. This is valid under the assumption that all energy is transferred to mechanical, considering this way that fluxes are constant (there in no back-emf), as well as stator and rotor currents [4].

$$T_e = -\frac{dW}{d\theta_m} = -p\frac{dW}{d\theta_d} = \tag{18}$$

$$= pM_f i_f \left[i_a \sin(\theta_d) + i_b \sin(\theta_d - 120^\circ) + i_c \sin(\theta_d - 240^\circ) \right]$$

Remaining equation used in active rectifier algorithm is the one that describes the mechanical subsystem:

$$J\frac{d\omega}{dt} = T_e - T_m - D_p(\omega - \omega_{grid})\,, \tag{19}$$

where J represents rotor moment of inertia, T_m is the load torque, whereas factor D_p models the damping effect, which mimics the existence of damping rotor winding. The moment of inertia value is a consequence of machine dimensions and this parameter increases with the machine size.

The final equation relevant for VSM is the one used for instantaneous reactive power calculation:

$$q = \frac{1}{\sqrt{3}}[i_a(u_b - u_c) + i_b(u_c - u_a) + i_c(u_a - u_b)] \tag{20}$$

In the following sections, it will be explained how the provided system of equations can be used to control a power converter as a VSM.

III. Virtual Synchronous Machine

Power converter controlled based on the mathematical model of a synchronous machine is considered a virtual synchronous machine, sometimes referred to as a synchronverter. Depending on the defined direction of grid currents, two main groups are distinguished, virtual synchronous generators (VSG) and virtual synchronous motors (VSM) [1]. One major difference is that VSMs require DC-bus voltage control to obtain the desired level of output voltage. On the other hand, VSGs are more oriented towards the active power flow and contain such controllers. In case of reactive

power control, the controller structure can be the same, but VSMs typically require average value of zero to achieve unity power factor.

Fig. 2 depicts structure of VSM, where the converter circuit and control block diagram of the system are highlighted. Further description is focused on each of enumerated parts of the block diagram and their main features [7].

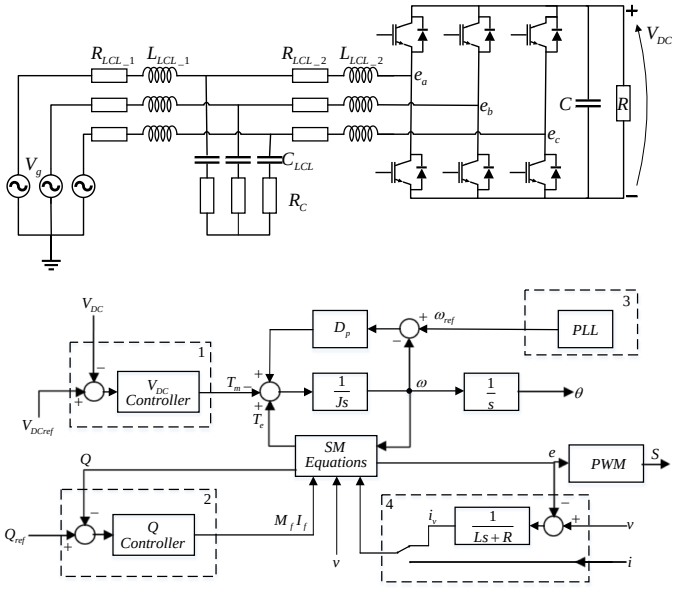

Fig. 2. Converter circuit (top) and block diagram of VSM algorithm (bottom)

A. Converter Circuit

Main components of an active rectifier are three phase transistor bridge, grid filter and DC bus capacitor. The resistor, connected in parallel with the DC-bus, represents rectifier load. Three legs of the bridge are connected to the grid which is represented as an ideal voltage source on one side, and to the output capacitor on the other side. Transistor commutation results in high frequency voltage which can not be safely coupled to the grid. Thus, the grid side filter, usually L, LC, or LCL type, is necessary for this application [3]. Analysis and selection of the type and rating of transistors for this kind of application, as well as the DC-bus capacitor bank, are more related to implementation and testing on real hardware. The effect of the grid-side filter on VSM performance and transient response will be the topic considered in this paper.

B. Grid-Side Filter

Due to PWM being carried out at frequencies several orders of magnitude higher than the grid voltage frequency, high-frequency current components are expected. In order to attenuate this part of the spectrum which could deteriorate grid characteristics when present at a higher scale, grid-side filter is used. Although the L type filter can lead to satisfactory results, reducing grid current ripple to acceptable level, the volume and potential cost of the inductor and its effects on converter dynamics are a major problem when high power applications are considered. Due to this, LCL filter presents a more acceptable solution to those problems [9]. The main disadvantage of LCL type filter is related to resonant peak. In the absence of a current controller, a passive solution is used for the given problem. Connecting a resistor in series with filter capacitor flattens the resonant peak and resolves this issue [10]. According to the research presented in [11], based on PWM frequency, current amplitude and allowed ripple as well as overall rated power of converter, parameters of LCL filter can be calculated.

Another aspect of grid filter parameter selection is that it acts as a series impedance of virtual synchronous machine stator. Real synchronous machine parameters depend on its dimensions and the winding structure. VSM allows to change these parameters in order to achieve better performance and desired response to load or reference change.

C. DC Voltage control

This controller maintains DC-bus voltage inside a narrow range around the desired value. The most common reasons for variations of DC-bus voltage are related to the change of rectifier load, grid voltage magnitude, or frequency fluctuation. For this application, PI controller is selected.

Difference between required and measured DC voltage is interpreted as an error and provided to PI controller block. The controller output represents the load torque. For the simplicity of the ongoing analysis, lets assume that the VSM frequency is constant and equal to the grid frequency and that the steady-state value of DC voltage is the same as the reference value. This simplification is justified by the fact that the DC-bus capacitance is relatively high and that the voltage ripple is negligible. Block diagram is presented in Fig. 3.

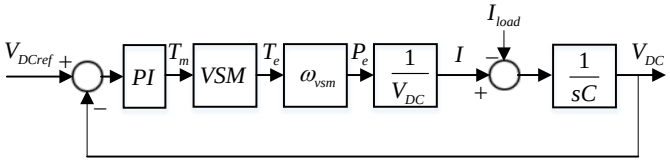

Fig. 3. Block diagram of DC control loop

VSM block describes the VSM electromagnetic torque response to certain load torque. It is mostly affected by the mechanical system parameters and LCL filter parameters. Since LCL filter is designed to improve grid current, the emphasis is on the effect of J and D_p values on the VSM response. Fig. 4 shows the effect of change of D_p on T_e when exposed to a step change of T_m.

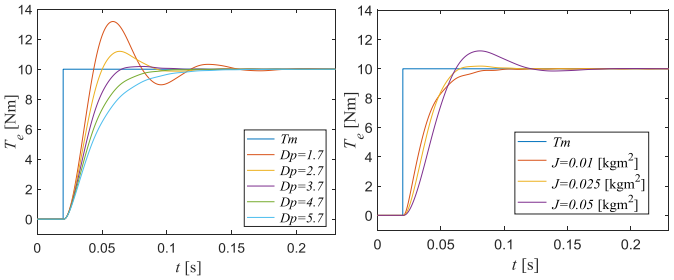

Fig. 4. Effects of different values of D_p with constant J (left) and different values of J with constant D_p on electromagnetic torque (right)

In a similar manner, for one selected value of D_p, it is possible to show how change in inertia affects VSM. It can be

seen that for certain pairs of values of D_p and J, the VSM acts as a first order system and its time constant can be determined. This allows easy PI controller parameters calculation, based on modulus optimum, due to reduction of closed loop transfer function order. It should be noted that increasing the moment of inertia results in improved stability for grid frequency disturbance, but at the cost of losing fast tracking of power reference change. A trade-off between these two goals must be performed. Alternatively, modifications to the VSG control must be introduced [12] to allow reference-tracking speed and virtual inertia to be set independently.

D. Reactive Power Control

In order to achieve unity power factor in a synchronous machine, the reactive power controller alters the excitation flux. In the case of VSM, the controller is an integrator with small-enough gain. Its input is reactive power error, and output is the excitation $M_f I_f$. Reactive power calculation is based on equation (20) from Section II.

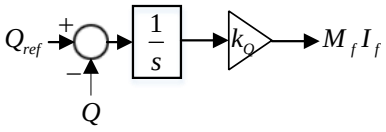

Fig. 5. Structure of reactive power controller

E. Phase Locked Loop

In order to synchronize VSM with grid voltage, PLL unit is used. PLL based on Park's transformation is described in [13] and the same one is used in this application, with additional Clarke transformation that is required to obtain 90 degrees phase shifted voltages. Block diagram which shows PLL structure is presented in Fig. 6. The main goal is to control the speed of the rotating reference frame in a manner that results in zero voltage value in the quadratic axis.

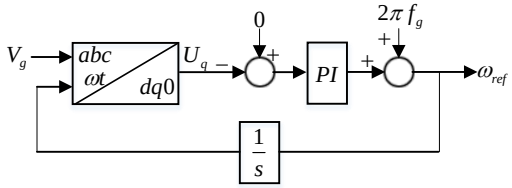

Fig. 6. Structure of PLL system

F. Grid Synchronization Block

When the contactor of VSM connects its terminals to the grid, a high current transient occurs. It is necessary to achieve PWM voltage reference in each phase as similar as possible to the grid voltage to avoid possible damage to the converter circuit. As a consequence, inrush currents become smaller in amplitude. One way of solving this issue is to use virtual impedance technique and its formulation is presented in (21),

$$i_v = \frac{u - e}{sL + R}, \tag{21}$$

where $sL+R$ is the virtual impedance [1]. Before connecting the converter to the grid, VSM algorithm is provided with virtual currents, calculated by difference between grid voltage and PWM reference signal divided by virtual impedance. DC-bus controller is disabled during this period in order to avoid additional torque in the virtual mechanical system. On the other hand, reactive power control helps to synchronize voltages amplitudes, while damper coefficient D_p acts as damper winding, synchronizing VSM frequency with the grid frequency. When the current is equal to zero for a certain period of time, VSM can be connected to the grid. Fig. 7 shows the difference in currents provided to the reactive power controller when synchronization algorithm is used and when it is not used. In the Fig. 7, on the left side, actual currents with direct connection to the grid, can be seen. Virtual currents can be seen in the first 0.3 seconds of the figure on the right. After that, once the currents are settled to a value near zero, converter is connected to the grid and actual currents are now provided to the VSM algorithm.

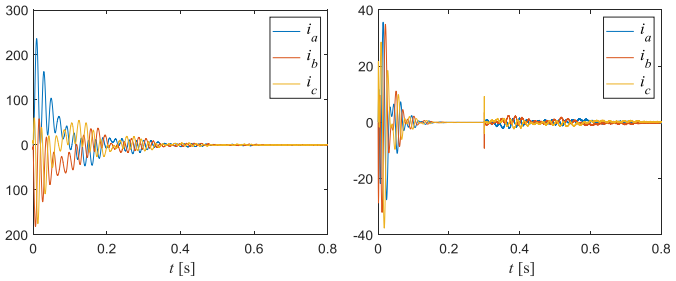

Fig. 7. Waveforms of currents i [A] brought to algorithm without (left) and with synchronization block (right)

IV. Real-Time Simulation Setup

Final step towards implementation of a grid-side converter as VSM is to create a hardware circuit, program a controller to execute provided algorithm, and supply PWM signals to transistor drivers. In order to avoid faults which could result in semiconductor breakdown or other damage, previous simulations are required. Software packages such as MATLAB Simulink can be used to verify controller parameters and overall stability of the designed system. However, simulations like those usually require a lot of time only to model transients in a span of several seconds. Moreover, changes of, say, load value or reference value, as well as contactor states, have to be determined previously. They will occur in specific moment during simulation, which is defined before running it. In addition, such simulations do not allow real-time implementation of control algorithm, therefore they cannot demonstrate the feasibility of the proposed controller in actual application.

Use of hardware-in-the-loop devices is an excellent way to evaluate the overall system performance in real time. That implies change of load, grid conditions, different gains of PI controllers, etc. It is important to emphasize that in this arrangement, displayed in Fig. 8 as an example, an actual control device is used.

From Fig. 8 it can also be seen that besides the Typhoon HIL 602+, which is the specific model of the used HIL device, a PED-Board is used for digital control of the simulated converter. The PED-Board is a controller board with National Instruments sbRIO-9651 device as its integral part. It is an

FPGA based „system on chip“. Programming is adapted to LabView software package. Both Typhoon HIL and PED-Board are recommended by their respective manufacturers for real-time grid converter verification.

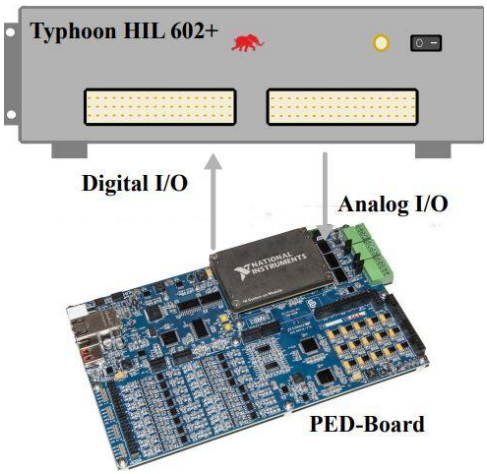

Fig. 8. Display of setup arrangement

Converter model is developed in Typhoon HIL Schematic Editor software and depicted in Fig. 9. Voltage and current measurements required by algorithm are available at devices analog outputs. These signals are scaled to a level of 5V, necessary for ADC circuitry of PED-Board and the custom-made adapter board. Once the sampling is performed, the VSM algorithm determines PWM switching signals, provided by PED-Board, and sends them to HIL device's digital inputs.

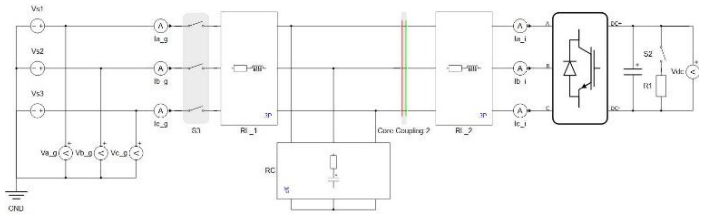

Fig. 9. Converter circuit model created in Typhoon HIL software

V. HIL SIMULATIONS RESULTS

VSM control algorithm developed in MATLAB Simulink environment has been verified using the previously described setup. As presented in Fig. 9, measurements that have been taken into account from the grid side are grid phase voltages and grid currents. It is assumed that grid voltages are balanced ideal 50 Hz sine waves without any additional harmonics. On the converter side, line-to-line voltages and phase currents are also measured. Besides that, DC-bus voltage has also been taken into account. Circuit parameters and controller gains are listed in Table I. Switching frequency is 10 kHz, as well as the sampling frequency. This leads to precise PWM switching considering the 40 MHz execution rate enabled by the PED-Board, which is sufficient for triangular wave generation.

Fig. 10 (left) displays three phase grid voltages. Based on their values, VSM algorithm calculates the sine wave references for PWM signal generation. Grid voltage and current of phase *a* are shown in Fig. 10 (right). It can clearly be seen that grid current is a sine wave function that is in phase with grid voltage. This means that the active rectifier creates voltages that result in approximately unity power factor. LCL filter is capable of reducing undesirable current ripple at the grid side. THD value of the grid current is 1.52%.

TABLE I. PARAMETERS OF VSM AND CONTROLLERS GAINS

Parameter	*Value*	*Parameter*	*Value*
V_{DC}	800 V	J	0.0025 kgm^2
C_{VDC}	1.1 mF	D_P	4.7 $\frac{\text{sNm}}{\text{rad}}$
R_{LCL1}	50 mΩ	K_{pPLL}	0.9
L_{LCL1}	1 mH	K_{iPLL}	1000
R_{LCL2}	50 mΩ	K_{pv}	0.0609
L_{LCL2}	7 mH	K_{iv}	0.6619
C_{LCL}	2.5 µF	K_{iQ}	0.0003125
R_C	10 Ω	f_{PWM}	10 kHz

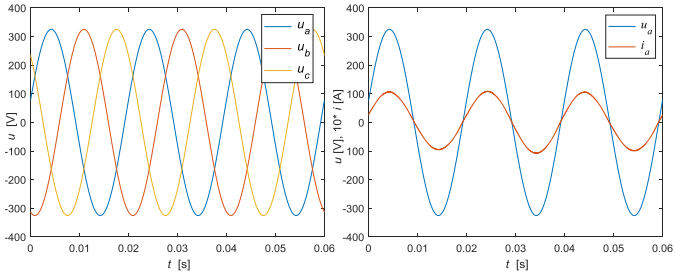

Fig. 10. Grid voltages (left), phase *a* current and voltage (right)

The performance of the active rectifier operated as a VSM is presented in Fig. 11. A test has been conducted in order to evaluate the performance of DC voltage regulation under various stress conditions. Fig. 11 (left) depicts how changes in DC voltage reference affect output DC voltage value. At first, after initial 800 V (for which the DC controller parameters are designed to operate) there was introduced a decrease that included two - 50 V steps. Then, an increase in reference which lead to 900 V was applied, followed by -200 V decrease in reference. Two additional + 50 V steps of reference change lead to desired 800 V output. It can be seen that the converter successfully achieved all of required values of DC reference. Fig. 11 (right) shows active and reactive power during voltage variation test. In addition, Fig. 12 (left) shows how rapid change in load, from 20% to 100% and vice versa affects DC voltage. During the test, DC voltage reference is set to 800 V. RMS value of the current in one of the phases, calculated in accordance with the grid frequency, is also presented. Fig. 12 (right) presents active and reactive power during the applied load variation test.

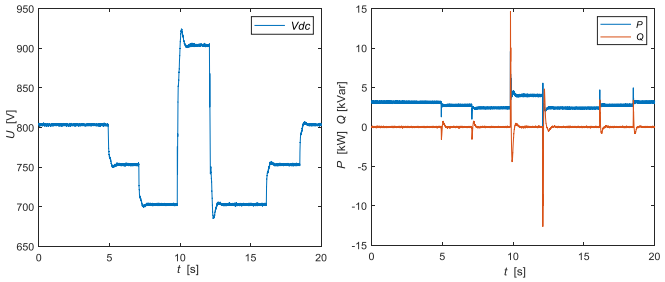

Fig. 11. Wide-range changes in DC voltage (left), active and reactive power during DC reference variation test (right)

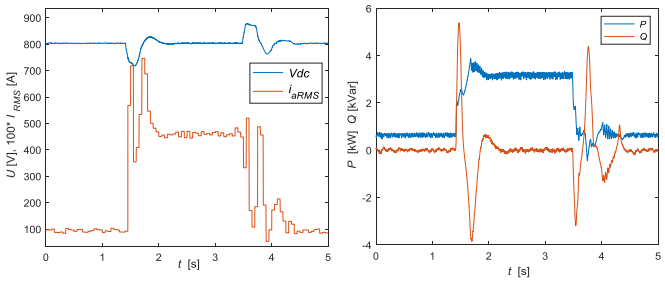

Fig. 12. Wide-range changes in load (left), active and reactive power during load variation test (right)

VI. Conclusion

An active rectifier controlled as a VSM was presented and implemented on a HIL platform. FPGA-based PED-Board controller was used to perform the proposed algorithm. It was shown that, with adequately set model and controller parameters, a required waveform of grid currents as well as DC-bus voltage value can simultaneously be obtained. During the HIL experiment, grid currents were in phase with voltages of respective phases, which lead to unity power factor operation of the converter. In addition, grid currents exhibited low level of ripple. Future research will be focused on the implementation of VSM on actual hardware in order to evaluate its performance in real-time grid defined conditions. Prior to that, PLL algorithm should be adapted to such conditions in which additional grid voltage harmonics and unbalance could occur and influence the control performance. Moreover, it is planned to investigate how implementation of a current controller affects the VSM converter performance.

Acknowledgment

This project has received funding from the European Union's HORIZON-WIDERA-2021-ACCESS-03 under grant agreement No 101079200. The authors also wish to thank Typhoon HIL for their support which made this work possible.

References

[1] Q. Zhong, "Virtual Synchronous Machines: A unified interface for grid integration", *IEEE Power Electronics Magazine*, vol.3, no. 4, pp. 18-27, Dec. 2016.

[2] P. Makolo, R. Zamora and L. Tek-Tjing, "The role of inertia for grid flexibility under high penetration of variable renewables - A review of challenges and solutions", *Renewable and Sustainable Energy Reviews* Volume 147,111223, ISSN 1364-0321, 2021.

[3] S. N. Vukosavic, "Grid-Side Converters Control and Design", *Springer*, 2018.

[4] Q. C. Zhong and G. Weiss, "Synchronverters: Inverters That Mimic Synchronous Generators", *IEEE Transactions on Industrial Electronics*, vol. 58, pp. 1259-1267,, April 2011.

[5] Y. Chen, R. Hesse, D. Turschner and H. Beck, "Improving the grid power quality using virtual synchronous machines", 2011 *International Conference on Power Engineering, Energy and Electrical Drives*,pp. 1-6, 2011.

[6] Myada Shadoul, Razzaqui Ahshan, Rashid Al Abri, Abdullah Al-badi and Mohammed Albadi, "A Comprehensive Review on a Virtual-Synchronous Generator: Topologies, Control Orders and Techniques, Energy Storages, and Applications", in *Energies. 15. 8406. 10.3390/en15228406*, 2022.

[7] Z. Ma, Q. C. Zhong and J. D. Yan, "Synchronverter-based control strategies for three-phase PWM rectifiers," in *7th IEEE Conference on Industrial Electronics and Applications (ICIEA), 2012, pp. 225-230*, 2012.

[8] J. J. Grainger and W. D. Stevenson, "Power system analysis", *New York: McGraw-Hill*, 1994.

[9] M. Liserre, F. Blaabjerg and S. Hansen, "Design and control of an LCL-filter-based three-phase active rectifier," *IEEE Transactions on Industry Application*, vol. 41, no. 5, pp. 1281-1291, 2005.

[10] R. Peña-Alzola, M. Liserre, F. Blaabjerg, R. Sebastian, J. Dannehl and F. W. Fuchs, "Analysis of the Passive Damping Losses in LCL-Filter-Based Grid Converters," *IEEE Transactions on Power Electronics*, vol. 28, no. 6, pp. 2642-2646, June 2013.

[11] DÖŞOĞLU, M. Dursun and K. M., "LCL Filter Design for Grid Connected Three-Phase Inverter," *2nd International Symposium on Multidisciplinary Studies and Innovative Technologies (ISMSIT), Ankara, Turkey,*, pp. 1-4, 2018.

[12] A. E. Leon and H. M. Mauricio, "Virtual Synchronous Generator for VSC-HVDC Stations With DC Voltage Control," *IEEE Transactions on Power Systems* , vol. 38, no. 1, pp. 728-738, 2023.

[13] R. Teodorescu, M. Liserre and P. Rodriguez, "Grid Converters for Photovoltaic and Wind Power Systems", *Wiley-IEEE Press*, 2007.